Journal of Physics Research and Education, Volume 3, March 2026

Comparative Observational Analysis of Barrow and Tsallis Holographic Dark Energy in Braneworld Models

Souvik Ghose*
High Energy and Cosmic Ray Research Centre,
University of North Bengal, Rajarammunpur 734015, India and
Harish-Chandra Research Institute, HBNI, Prayagraj, 211019, India

We perform a comparative observational analysis of Barrow and Tsallis holographic dark energy models within the framework of braneworld cosmology. Working in the Dvali–Gabadadze–Porrati (DGP) and Randall–Sundrum type II (RSII) scenarios, we consider the Hubble horizon as the infrared cutoff and constrain the models using Observed Hubble Data (OHD). Building upon earlier dynamical studies and a preliminary observational analysis of Barrow holographic dark energy, we employ a Bayesian Markov Chain Monte Carlo approach to obtain marginalized posterior distributions, confidence intervals and parameter correlations. Our results show that the Barrow holographic dark energy model yields well-constrained deformation parameters in both DGP and RSII braneworlds, consistent with their theoretical bounds and exhibiting weak parameter degeneracies. In contrast, while the Tsallis holographic dark energy provides an acceptable fit to the OHD data, its normalization parameter remains weakly constrained, and the preferred values of the Tsallis exponent differ significantly from those commonly adopted in earlier dynamical analyses. These results indicate that observational constraints favor the Barrow formulation over the Tsallis one within the braneworld context considered here, and thereby highlighting the role of theoretical entropy bounds in improving the robustness of holographic dark energy models.

I. INTRODUCTION

Observational evidence from Type Ia supernovae, cosmic microwave background anisotropies, and large-scale structure surveys indicates that the Universe is presently undergoing a phase of accelerated expansion [1–4]. Although the cosmological constant within General Relativity provides a phenomenologically successful explanation, its extreme fine-tuning and coincidence problems continue to motivate alternative approaches [5, 6]. Among the proposed alternatives, braneworld cosmology offers a compelling geometric modification of gravitational dynamics, in which our observable Universe is realized as a four-dimensional brane embedded in a higher-dimensional bulk [7, 8]. In particular, the Dvali–Gabadadze–Porrati (DGP) model [9] and the Randall–Sundrum type II (RSII) scenario [8] modify the effective Friedmann equations and can significantly alter late-time cosmological evolution. While the self-accelerating branch of the DGP model suffers from ghost instabilities [10], the normal branch remains viable provided a dark energy component is present. Similarly, RSII cosmology generally requires an explicit dark energy sector to account for the observed acceleration.

* dr.souvikghose@gmail.com

Holographic Dark Energy (HDE) is motivated by the holographic principle [11, 12] and the entropy bound proposed by Cohen, Kaplan and Nelson [13], which relates the ultraviolet cutoff of a quantum field theory to an infrared scale determined by black-hole formation. The resulting dark energy density takes the form $\rho_{\rm DE} \propto L^{-2}$, where L is an infrared cutoff. However, as pointed out by Hsu [14], standard HDE fails to produce late-time acceleration when the Hubble horizon is chosen as the infrared cutoff within General Relativity. This shortcoming has motivated several generalized holographic models based on modified entropy formalisms. One such generalization is Tsallis Holographic Dark Energy (THDE), constructed using the non-additive Tsallis entropy [15]. The cosmological implications of THDE have been studied extensively in various gravitational frameworks [16, 17]. In particular, Ghaffari *et al.* [17] demonstrated that THDE can successfully describe the cosmic evolution in both DGP and RSII braneworld scenarios when the Hubble radius is employed as the infrared cutoff.

Recently, Barrow proposed a deformation of the Bekenstein–Hawking entropy motivated by possible quantum-gravitational fractal structures of black-hole horizons [18]. This modification leads to Barrow Holographic Dark Energy (BHDE), characterized by a deformation parameter that is theoretically constrained. The cosmological behavior of BHDE has been explored in standard cosmology and subsequently in braneworld scenarios, where it was shown that BHDE can reproduce late-time acceleration and asymptotic ΛCDM behavior under appropriate conditions. A recent analysis investigated BHDE in the DGP and RSII braneworld frameworks using the Hubble horizon as the infrared cutoff and demonstrated its dynamical viability, stability properties, and preliminary observational consistency with Observed Hubble Data [19]. While this study established the basic phenomenological success of BHDE in braneworld cosmology, the observational analysis was necessarily limited in scope and did not include a statistically robust parameter estimation or confidence interval construction.

The motivation of the present work is to extend these earlier investigations by performing a systematic Bayesian parameter estimation of both Barrow and Tsallis holographic dark energy models within identical DGP and RSII braneworld settings. Using recent Observed Hubble Data and Markov Chain Monte Carlo techniques, we aim to constrain the model parameters, construct confidence regions, and assess the relative observational viability of the two generalized holographic dark energy formulations. This comparative approach allows us to examine whether the theoretically constrained Barrow entropy leads to a more robust realization of holographic dark energy when confronted with observational data.

II. THEORETICAL FRAMEWORK

In this section, we briefly summarize the theoretical ingredients required for the present analysis. All models discussed below have been studied in detail in the literature and in Ref. [19]. Here we only outline the essential definitions and equations relevant for parameter estimation.

A. Holographic Dark Energy

Holographic Dark Energy (HDE) is motivated by the holographic principle, which relates the ultraviolet (UV) cutoff of a quantum field theory to an infrared (IR) cutoff due to black-hole formation. Imposing the condition that the total vacuum energy inside a region of size L should

not exceed the mass of a black hole of the same size leads to

$$\rho_{\rm DE} \leq 3c^2 M_{\rm pl}^2 L^{-2}, \tag{1}$$

where c is a dimensionless constant, $M_{\rm pl}$ is the reduced Planck mass and L denotes the infrared cutoff. In standard HDE, choosing the Hubble horizon $L = H^{-1}$ fails to produce late-time acceleration within General Relativity. This motivates generalized holographic models based on modified entropy formalisms.

B. Tsallis Holographic Dark Energy

Tsallis Holographic Dark Energy (THDE) is based on the non-additive Tsallis entropy, given by

$$S_T = \gamma A^{\delta}, \tag{2}$$

where A is the horizon area, δ is the Tsallis parameter and γ is a constant. Using this entropy in the holographic argument leads to the THDE energy density:

$$\rho_{\rm THDE} = BL^{2\delta-4}, \tag{3}$$

where B is a model-dependent constant. For $\delta = 1$, THDE reduces to standard HDE. In this work, as in earlier studies, the Hubble horizon $L = H^{-1}$ is chosen as the infrared cutoff.

C. Barrow Holographic Dark Energy

Barrow Holographic Dark Energy (BHDE) originates from a deformation of the Bekenstein–Hawking entropy due to possible quantum-gravitational fractal features of the black-hole horizon. The modified entropy is expressed as,

$$S_B = \left(\frac{A}{A_0}\right)^{1+\Delta/2}, \tag{4}$$

where A is the horizon area, A_0 is the Planck area and Δ ($0 \leq \Delta \leq 1$) is the Barrow exponent measuring the degree of deformation. Employing this entropy in the holographic framework yields the BHDE energy density

$$\rho_{\rm BHDE} = CL^{\Delta-2}, \tag{5}$$

where C is a constant with appropriate dimensions. As in the THDE case, we adopt the Hubble horizon $L = H^{-1}$ as the infrared cutoff.

D. DGP Braneworld Cosmology

In the Dvali–Gabadadze–Porrati (DGP) braneworld model, a four-dimensional brane is embedded in a five-dimensional Minkowski bulk. The modified Friedmann equation for a spatially flat

universe is given as,

$$H^2 - \frac{\epsilon}{r_c} H = \frac{\rho}{3M_{\rm pl}^2}, \tag{6}$$

where ρ is the total energy density on the brane, r_c is the crossover scale and $\epsilon = \pm 1$ distinguishes the two branches of the solution. In this work, we focus on the normal branch ($\epsilon = -1$), which requires a dark energy component to drive late-time acceleration.

E. RSII Braneworld Cosmology

In the Randall–Sundrum type II (RSII) scenario, the Universe is a four-dimensional brane embedded in a five-dimensional Anti-de Sitter bulk. The effective Friedmann equation on the brane can be written as,

$$H^2 = \frac{8\pi}{3M_{\rm pl}^2} \left(\rho_m + \rho_{\rm DE}\right), \tag{7}$$

where ρ_m denotes the pressureless matter density and $\rho_{\rm DE}$ represents the effective dark energy density induced on the brane. For large horizon scales, the dominant contribution to $\rho_{\rm DE}$ arises from the holographic dark energy sector, which we model using either BHDE or THDE.

F. Energy Conservation

Throughout this work, we assume no interaction between dark matter and dark energy. The conservation equations therefore take the standard form:

$$\dot{\rho}_m + 3H\rho_m = 0 \tag{8}$$

$$\dot{\rho}_{\rm DE} + 3H(1+\omega_{\rm DE})\rho_{\rm DE} = 0, \tag{9}$$

where $\omega_{\rm DE}$ is the equation-of-state parameter of the dark energy component. This theoretical framework forms the basis for the observational analysis presented in the subsequent sections.

III. METHODOLOGY: PARAMETER ESTIMATION WITH OBSERVED HUBBLE DATA

In order to constrain the Barrow and Tsallis holographic dark energy models in the DGP and RSII braneworld frameworks, we perform a Bayesian parameter estimation using Observed Hubble Data (OHD). The analysis is carried out via Markov Chain Monte Carlo (MCMC) techniques implemented through the `emcee` Python package.

A. Observed Hubble Data

The dataset used in this work consists of measurements of the Hubble parameter $H(z)$ at different redshifts, commonly referred to as Observed Hubble Data. These measurements are primarily obtained using the cosmic chronometer (differential age) method, with a smaller subset derived from complementary techniques. Each data point is characterized by an observed value $H_{\rm obs}(z_i)$ and an associated uncertainty σ_i. Since OHD directly probes the expansion history of the Universe

without assuming a specific background cosmology, it provides a robust dataset for constraining dark energy models.

B. Theoretical Model

For a given cosmological scenario (BHDE or THDE in DGP or RSII braneworld), the theoretical Hubble parameter $H_{\rm th}(z;\boldsymbol{\theta})$ is obtained by numerically solving the corresponding modified Friedmann equations. Here, $\boldsymbol{\theta}$ denotes the set of free model parameters, which include the holographic deformation parameter (the Barrow exponent Δ or the Tsallis parameter δ) along with any additional parameters required by the specific braneworld framework. The theoretical predictions are evaluated at the same redshifts as the observational data.

C. Likelihood Function

Following the standard prescription described in the `emcee` tutorial for line fitting, we assume a Gaussian likelihood with an additional nuisance parameter f that accounts for possible underestimation of observational uncertainties or intrinsic scatter. The log-likelihood function is given by,

$$\ln \mathcal{L}(\boldsymbol{\theta}, f) = -\frac{1}{2}\sum_i \left[\frac{\left(H_{\rm obs}(z_i) - H_{\rm th}(z_i;\boldsymbol{\theta})\right)^2}{\sigma_i^2 + f^2 H_{\rm th}^2(z_i;\boldsymbol{\theta})} + \ln\left(\sigma_i^2 + f^2 H_{\rm th}^2(z_i;\boldsymbol{\theta})\right) \right]. \tag{10}$$

The nuisance parameter f is treated as a free parameter and is marginalized over in the MCMC analysis.

D. Expressions for the Hubble Parameter

The following expressions are used to constrain the models. Relevant descriptions and derivations of these equations can be found in [19, 20]. For
BHDE in DGP:

$$\frac{\dot{H}}{H^2} = -\frac{3\left(1-\Omega_D - 2\epsilon\sqrt{\Omega_{r_c}}\right)}{(\Delta-2)\Omega_D - 2\epsilon\sqrt{\Omega_{r_c}} + 2}. \tag{11}$$

BHDE in RSII:

$$\frac{\dot{H}}{H^2} = \frac{3(\Omega_\Lambda - 1)}{2 + (\Delta-2)\Omega_\Lambda}. \tag{12}$$

THDE in DGP:

$$\frac{\dot{H}}{H^2} = -\frac{3\left(1-\Omega_D - 2\epsilon\sqrt{\Omega_{r_c}}\right)}{2(\delta-2)\Omega_D - 2\epsilon\sqrt{\Omega_{r_c}} + 2}. \tag{13}$$

THDE in RSII:

$$\frac{\dot{H}}{H^2} = \frac{3(2\Omega_\Lambda - 1)}{1 + 2\Omega_\Lambda(\delta-2)}. \tag{14}$$

These equations can be solved to obtain the value of the Hubble parameter at any redshift and for any of the models (i.e. $H_{\rm th}$).

E. Priors

Gaussian priors are imposed on all model parameters. The Barrow exponent Δ is restricted to its theoretically allowed range, while the Tsallis parameter δ is allowed to vary within a range motivated by previous observational studies. The nuisance parameter f is assigned a Gaussian prior centered at zero with a sufficiently large variance to avoid biasing the parameter estimation. The total log-posterior probability is constructed as the sum of the log-likelihood and the log-priors.

F. MCMC Implementation

Sampling of the posterior distribution is performed using the affine-invariant ensemble sampler implemented in the `emcee` package. An ensemble of walkers is initialized around reasonable initial values in parameter space. After discarding an initial burn-in phase, the chains are evolved until convergence is achieved, as verified through inspection of trace plots and stability of the posterior distributions. Final parameter estimates are obtained from the marginalized posterior distributions, with best-fit values reported as the median and uncertainties quoted at the 68%, 95%, and 99% credible levels.

IV. RESULTS

A. BHDE in DGP Braneworld: Constraints from OHD

We first present the observational constraints on the Barrow Holographic Dark Energy (BHDE) model in the DGP braneworld scenario obtained using Observed Hubble Data. The analysis is carried out on the normal branch of the DGP model, with the Hubble horizon chosen as the infrared cutoff and assuming no interaction between dark matter and dark energy. The free parameters in this model are the BHDE parameter c, the Barrow exponent Δ, and the nuisance parameter $\log(f)$ introduced in the likelihood to account for possible intrinsic scatter. The posterior distributions are obtained using the MCMC methodology described in the previous section. The marginalized parameter constraints at the 68% confidence level are

$$c = 53.057^{+0.298}_{-0.301}, \tag{15}$$

$$\Delta = 0.686^{+0.079}_{-0.079}, \tag{16}$$

$$\log(f) = -0.201^{+0.105}_{-0.099}. \tag{17}$$

The corresponding covariance matrix for the parameters $(c,\ \Delta,\ \log f)$ is

$$\mathrm{Cov} = \begin{pmatrix} 0.0878 & 0.00032 & 0.00042 \\ 0.00032 & 0.00646 & -0.00016 \\ 0.00042 & -0.00016 & 0.01066 \end{pmatrix}. \tag{18}$$

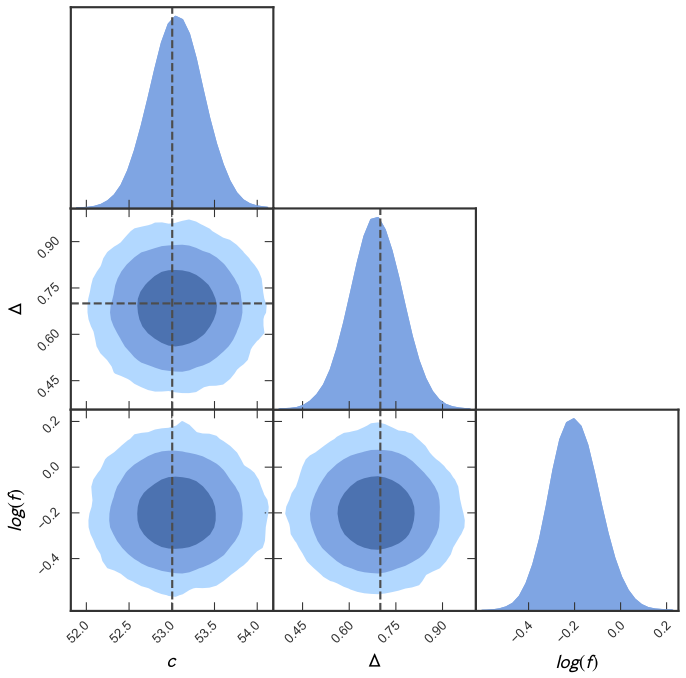

FIG. 1. Corner plot showing the marginalized posterior distributions and joint confidence contours for the BHDE parameters c, Δ, and $\log(f)$ in the DGP braneworld model, obtained from Observed Hubble Data. The contours correspond to the 68%, 95%, and 99% confidence levels.

The relatively small off-diagonal elements indicate that the parameters are only weakly correlated, suggesting that the OHD data are capable of constraining the BHDE parameter Δ largely independently of the normalization parameter c and the nuisance parameter $\log(f)$. This strengthens the robustness of the inferred constraint on the Barrow exponent. Figure (1) shows the marginalized posterior distributions and joint confidence contours for $(c,\ \Delta,\ \log f)$, generated using the `pygtc` package. The contours correspond to three confidence levels (typically 68%, 95%, and 99%), providing a clear visualization of the parameter degeneracies and uncertainties. The posterior distributions are well behaved and approximately Gaussian, with no evidence of multimodality. The best-fit value of the Barrow exponent lies well within its theoretically allowed range $0 \leqslant \Delta \leqslant 1$ and exhibits a significant deviation from the standard holographic limit $\Delta = 0$. This indicates that the OHD data favor a nontrivial Barrow deformation in the DGP braneworld scenario. The nuisance parameter $\log(f)$ remains close to zero, implying that the quoted observational uncertainties are largely sufficient and that no substantial additional variance is required by the model. Overall, these results demonstrate that BHDE provides an excellent fit to the OHD data in the DGP braneworld framework and supports a consistent, observationally viable departure from standard holographic dark energy.

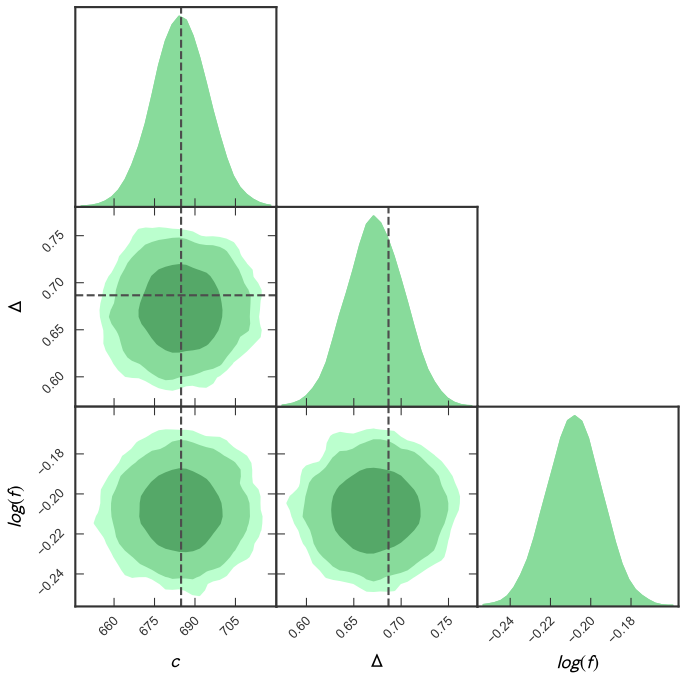

FIG. 2. Corner plot showing the marginalized posterior distributions and joint confidence contours for the BHDE parameters c, Δ, and $\log(f)$ in the RSII braneworld model, obtained from Observed Hubble Data. The contours correspond to the 68%, 95%, and 99% confidence levels.

B. BHDE in RSII Braneworld: Constraints from OHD

We now present the observational constraints on the Barrow Holographic Dark Energy (BHDE) model in the RSII braneworld scenario obtained using Observed Hubble Data. As in the DGP case, the Hubble horizon is chosen as the infrared cutoff, and no interaction between dark matter and dark energy is assumed. The free parameters of the model are the BHDE normalization parameter c, the Barrow exponent Δ, and the nuisance parameter $\log(f)$. The marginalized constraints at the 68% confidence level are found to be

$$c = 684.589^{+9.968}_{-9.814}, \tag{19}$$

$$\Delta = 0.673^{+0.030}_{-0.030}, \tag{20}$$

$$\log(f) = -0.208^{+0.013}_{-0.013}. \tag{21}$$

The correlation matrix for the parameters $(\Delta,\, c,\, \log f)$ is given by,

$$\mathrm{Corr} = \begin{pmatrix} 1.000 & 0.012 & 0.003 \\ 0.012 & 1.000 & 0.021 \\ 0.003 & 0.021 & 1.000 \end{pmatrix}. \tag{22}$$

The small off-diagonal elements indicate that the parameters are only very weakly correlated. In particular, the Barrow exponent Δ is essentially uncorrelated with both the normalization parame-

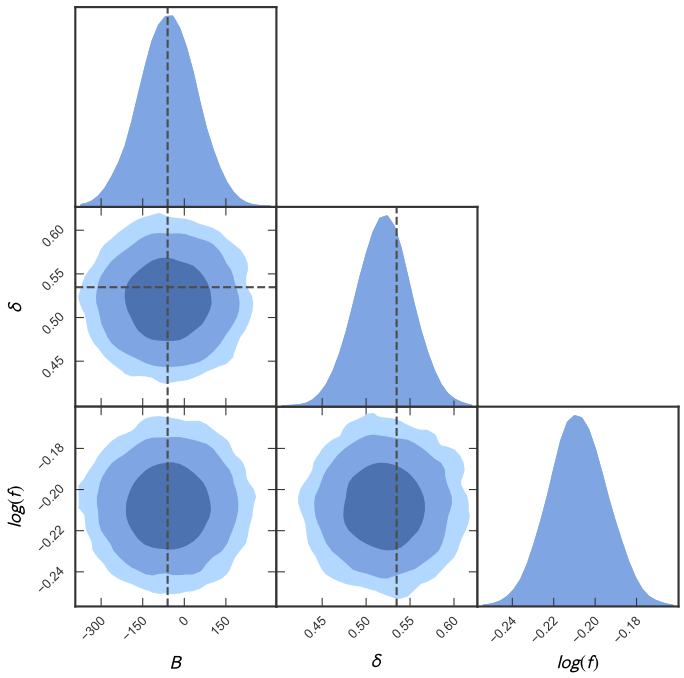

FIG. 3. Corner plot showing the marginalized posterior distributions and joint confidence contours for the THDE parameters B, δ, and $\log(f)$ in the DGP braneworld model, obtained from Observed Hubble Data. The contours correspond to the 68%, 95%, and 99% confidence levels.

ter c and the nuisance parameter $\log(f)$, demonstrating that the RSII braneworld framework allows for a clean and independent determination of the Barrow deformation from OHD. The marginalized posterior distributions and joint confidence contours for $(c,\ \Delta,\ \log f)$ are shown in Fig. (2). The contours correspond to three confidence levels and exhibit smooth, unimodal, and approximately Gaussian behavior, with no evidence of significant degeneracies or multimodality. The posterior for Δ is notably tighter than in the DGP case, indicating that OHD constrains the Barrow exponent more stringently in the RSII braneworld scenario. The best-fit value of the Barrow exponent again lies well within its theoretically allowed range $0 \leqslant \Delta \leqslant 1$ and shows a clear preference for a nonzero deformation, reinforcing the consistency of BHDE with observational data in the RSII framework. The nuisance parameter $\log(f)$ remains close to zero, suggesting that the observational uncertainties adequately describe the data without requiring substantial additional scatter. Overall, these results confirm that BHDE provides an excellent and statistically robust description of the OHD data in the RSII braneworld model, with tighter constraints and weaker parameter degeneracies compared to the DGP case.

C. THDE in DGP Braneworld: Constraints from OHD

We now present the observational constraints on the Tsallis Holographic Dark Energy (THDE) model in the DGP braneworld scenario obtained using Observed Hubble Data. As in the previous analyses, the normal branch of the DGP model is considered, the Hubble horizon is adopted as

the infrared cutoff, and no interaction between dark matter and dark energy is assumed. The free parameters of the THDE model are the normalization parameter B, the Tsallis exponent δ, and the nuisance parameter $\log(f)$. The marginalized constraints at the 68% confidence level are found to be

$$B = -57.390^{+97.606}_{-99.649}, \tag{23}$$

$$\delta = 0.520^{+0.030}_{-0.030}, \tag{24}$$

$$\log(f) = -0.208^{+0.014}_{-0.013}. \tag{25}$$

The corresponding correlation matrix for the parameters $(\delta,\ B,\ \log f)$ is given by

$$\mathrm{Corr} = \begin{pmatrix} 1.000 & 0.016 & 0.020 \\ 0.016 & 1.000 & -0.007 \\ 0.020 & -0.007 & 1.000 \end{pmatrix}. \tag{26}$$

The small off-diagonal elements indicate that the parameters exhibit only weak mutual correlations. In particular, the Tsallis exponent δ is only mildly correlated with both the normalization parameter B and the nuisance parameter $\log(f)$, implying that the large uncertainty in B is not driven by parameter degeneracy but rather by the limited sensitivity of OHD to this parameter. The marginalized posterior distributions and joint confidence contours for the THDE parameters are shown in Fig. (3). The posteriors are smooth and unimodal, with approximately Gaussian profiles. While the Tsallis exponent δ is tightly constrained, the normalization parameter B remains weakly constrained, exhibiting a broad posterior distribution that spans both positive and negative values. This behavior is expected, as Observed Hubble Data primarily constrain the redshift evolution of the expansion rate rather than its absolute normalization.

Notably, the best-fit value of the Tsallis exponent obtained here differs significantly from values commonly adopted in earlier dynamical studies. In particular, Ghaffari *et al.* [20] demonstrated that THDE can successfully model the cosmological evolution in the DGP braneworld for δ in the range $2.22 \lesssim \delta \lesssim 2.46$. The present OHD-based analysis, however, favors a substantially lower value of δ, suggesting that observational constraints may point toward a different region of the parameter space than that typically explored in purely dynamical analyses. The nuisance parameter $\log(f)$ remains close to zero, indicating that the quoted observational uncertainties adequately describe the data without requiring significant additional scatter. Overall, while THDE provides an acceptable fit to the OHD data in the DGP braneworld scenario, the weak constraint on the normalization parameter and the preference for a lower Tsallis exponent highlight important differences with respect to the BHDE case, which will be discussed further in the comparative analysis.

D. THDE in RSII Braneworld: Constraints from OHD

We finally present the observational constraints on the Tsallis Holographic Dark Energy (THDE) model in the RSII braneworld scenario using Observed Hubble Data. As in the previous analyses, the Hubble horizon is chosen as the infrared cutoff, and no interaction between dark matter and dark energy is assumed. The free parameters of the THDE model in the RSII framework are the normalization parameter B, the Tsallis exponent δ, and the nuisance parameter

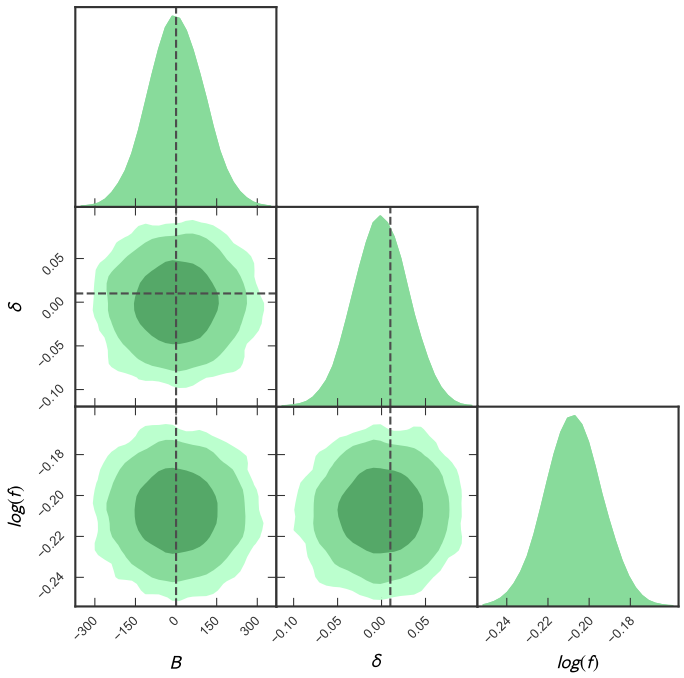

FIG. 4. Corner plot showing the marginalized posterior distributions and joint confidence contours for the THDE parameters B, δ, and $\log(f)$ in the RSII braneworld model, obtained from Observed Hubble Data. The contours correspond to the 68%, 95%, and 99% confidence levels.

$\log(f)$. The marginalized constraints at the 68% confidence level are obtained as

$$B = -0.086^{+100.980}_{-98.121}, \tag{27}$$

$$\delta = 0.001^{+0.030}_{-0.030}, \tag{28}$$

$$\log(f) = -0.208^{+0.013}_{-0.013}. \tag{29}$$

The corresponding correlation matrix for the parameters $(\delta,\ B,\ \log f)$ is

$$\mathrm{Corr} = \begin{pmatrix} 1.000 & 0.003607 & -0.014515 \\ 0.003607 & 1.000 & 0.015460 \\ -0.014515 & 0.015460 & 1.000 \end{pmatrix}. \tag{30}$$

As in the DGP case, the off-diagonal elements of the correlation matrix are small, indicating that the parameters are only weakly correlated. In particular, the Tsallis exponent δ is effectively uncorrelated with the normalization parameter B, implying that the large uncertainty in B is not caused by parameter degeneracy but rather reflects the limited sensitivity of OHD to the overall normalization of the dark energy density. The marginalized posterior distributions and joint confidence contours for the THDE parameters in the RSII braneworld are shown in Fig. (4). The posteriors are smooth, unimodal, and approximately Gaussian. While the Tsallis exponent δ is tightly constrained, the normalization parameter B remains weakly constrained and exhibits a broad posterior distribution. This behavior is similar to that observed in the DGP framework and again highlights

the limited constraining power of OHD on normalization parameters.

It is noteworthy that the best-fit value of the Tsallis exponent obtained here differs substantially from the parameter range typically adopted in earlier dynamical studies. In particular, Ghaffari *et al.* [20] demonstrated that THDE can successfully describe the cosmological evolution in the RSII braneworld for significantly larger values of the Tsallis exponent, typically in the range $3.2 \lesssim \delta \lesssim 3.6$. The present OHD-based analysis instead favors a much lower value of δ, suggesting that observational constraints may point toward a different region of the THDE parameter space than that explored in background-level dynamical analyses. The nuisance parameter $\log(f)$ remains close to zero, indicating that the quoted observational uncertainties adequately account for the scatter in the data. Overall, while THDE provides an acceptable fit to the OHD data in the RSII braneworld scenario, the weak constraint on the normalization parameter and the preference for a low Tsallis exponent closely mirror the behavior found in the DGP case and stand in contrast to the tighter and more theoretically restricted constraints obtained for BHDE.

V. CONCLUSION

In this work, we have carried out a systematic observational comparison of Barrow and Tsallis holographic dark energy models in DGP and RSII braneworld cosmologies using Observed Hubble Data. Taking a recent study of Barrow holographic dark energy as the starting point, we extended the analysis by performing full Bayesian parameter estimation, constructing confidence intervals, and examining parameter correlations within a unified statistical framework. Our results show that Barrow holographic dark energy leads to tightly constrained deformation parameters in both braneworld scenarios, with values lying well within their theoretically allowed range and exhibiting weak correlations with other model parameters. The constraints are particularly strong in the RSII framework, indicating that the Barrow deformation can be robustly determined from OHD alone. In contrast, although the Tsallis holographic dark energy provides an acceptable description of the expansion history, its normalization parameter remains weakly constrained in both the DGP and RSII scenarios. Moreover, the OHD-based analysis favors the Tsallis exponent values significantly lower than those typically employed in earlier background-level dynamical studies.

These findings suggest that, within the braneworld frameworks considered here and for the Hubble horizon as the infrared cutoff, the theoretically constrained Barrow entropy formulation offers a more robust and observationally stable realization of holographic dark energy than the Tsallis formulation. Future work incorporating additional datasets, such as supernovae or baryon acoustic oscillations, may further clarify the observational viability and discriminating power of generalized holographic dark energy models.

[1] A. G. Riess *et al.*, Astron. J. **116**, 1009 (1998).
[2] S. Perlmutter *et al.*, Astrophys. J. **517**, 565 (1999).
[3] D. N. Spergel *et al.*, Astrophys. J. Suppl. **148**, 175 (2003).
[4] N. Aghanim *et al.* (Planck Collaboration), Astron. Astrophys. **641**, A6 (2020).
[5] S. Weinberg, Rev. Mod. Phys. **61**, 1 (1989).
[6] T. Padmanabhan, Phys. Rept. **380**, 235 (2003).

[7] L. Randall and R. Sundrum, Phys. Rev. Lett. **83**, 3370 (1999).
[8] L. Randall and R. Sundrum, Phys. Rev. Lett. **83**, 4690 (1999).
[9] G. R. Dvali, G. Gabadadze and M. Porrati, Phys. Lett. B **485**, 208 (2000).
[10] M. A. Luty, M. Porrati and R. Rattazzi, JHEP **09**, 029 (2003).
[11] G. 't Hooft, gr-qc/9310026.
[12] L. Susskind, J. Math. Phys. **36**, 6377 (1995).
[13] A. G. Cohen, D. B. Kaplan and A. E. Nelson, Phys. Rev. Lett. **82**, 4971 (1999).
[14] S. D. H. Hsu, Phys. Lett. B **594**, 13 (2004).
[15] C. Tsallis, J. Stat. Phys. **52**, 479 (1988).
[16] M. Tavayef *et al.*, Phys. Lett. B **781**, 195 (2018).
[17] S. Ghaffari *et al.*, Phys. Lett. B **781**, 182 (2018).
[18] J. D. Barrow, Phys. Lett. B **808**, 135643 (2020).
[19] A. Chanda, *et al.*, Class. Quant. Grav. **41**, 035004 (2024).
[20] S. Ghaffari *et al.*, Phys. Dark Univ. **23**, 100246 (2019).